FERMILAB-CONF-06-164-E

Measurement of the $t\bar{t}$ Production Cross Section in $p\bar{p}$ Collisions at $\sqrt{s} = 1.96$ TeV

A. Abulencia,[23] D. Acosta,[17] J. Adelman,[13] T. Affolder,[10] T. Akimoto,[55] M.G. Albrow,[16] D. Ambrose,[16] S. Amerio,[43] D. Amidei,[34] A. Anastassov,[52] K. Anikeev,[16] A. Annovi,[18] J. Antos,[1] M. Aoki,[55] G. Apollinari,[16] J.-F. Arguin,[33] T. Arisawa,[57] A. Artikov,[14] W. Ashmanskas,[16] A. Attal,[8] F. Azfar,[42] P. Azzi-Bacchetta,[43] P. Azzurri,[46] N. Bacchetta,[43] H. Bachacou,[28] W. Badgett,[16] A. Barbaro-Galtieri,[28] V.E. Barnes,[48] B.A. Barnett,[24] S. Baroiant,[7] V. Bartsch,[30] G. Bauer,[32] F. Bedeschi,[46] S. Behari,[24] S. Belforte,[54] G. Bellettini,[46] J. Bellinger,[59] A. Belloni,[32] E. Ben Haim,[44] D. Benjamin,[15] A. Beretvas,[16] J. Beringer,[28] T. Berry,[29] A. Bhatti,[50] M. Binkley,[16] D. Bisello,[43] R. E. Blair,[2] C. Blocker,[6] B. Blumenfeld,[24] A. Bocci,[15] A. Bodek,[49] V. Boisvert,[49] G. Bolla,[48] A. Bolshov,[32] D. Bortoletto,[48] J. Boudreau,[47] A. Boveia,[10] B. Brau,[10] C. Bromberg,[35] E. Brubaker,[13] J. Budagov,[14] H.S. Budd,[49] S. Budd,[23] K. Burkett,[16] G. Busetto,[43] P. Bussey,[20] K. L. Byrum,[2] S. Cabrera,[15] M. Campanelli,[19] M. Campbell,[34] F. Canelli,[8] A. Canepa,[48] D. Carlsmith,[59] R. Carosi,[46] S. Carron,[15] M. Casarsa,[54] A. Castro,[5] P. Catastini,[46] D. Cauz,[54] M. Cavalli-Sforza,[3] A. Cerri,[28] L. Cerrito,[42] S.H. Chang,[27] J. Chapman,[34] Y.C. Chen,[1] M. Chertok,[7] G. Chiarelli,[46] G. Chlachidze,[14] F. Chlebana,[16] I. Cho,[27] K. Cho,[27] D. Chokheli,[14] J.P. Chou,[21] P.H. Chu,[23] S.H. Chuang,[59] K. Chung,[12] W.H. Chung,[59] Y.S. Chung,[49] M. Ciljak,[46] C.I. Ciobanu,[23] M.A. Ciocci,[46] A. Clark,[19] D. Clark,[6] M. Coca,[15] G. Compostella,[43] M.E. Convery,[50] J. Conway,[7] B. Cooper,[30] K. Copic,[34] M. Cordelli,[18] G. Cortiana,[43] F. Cresciolo,[46] A. Cruz,[17] C. Cuenca Almenar,[7] J. Cuevas,[11] R. Culbertson,[16] D. Cyr,[59] S. DaRonco,[43] S. D'Auria,[20] M. D'Onofrio,[3] D. Dagenhart,[6] P. de Barbaro,[49] S. De Cecco,[51] A. Deisher,[28] G. De Lentdecker,[49] M. Dell'Orso,[46] F. Delli Paoli,[43] S. Demers,[49] L. Demortier,[50] J. Deng,[15] M. Deninno,[5] D. De Pedis,[51] P.F. Derwent,[16] C. Dionisi,[51] J.R. Dittmann,[4] P. DiTuro,[52] C. Dörr,[25] S. Donati,[46] M. Donega,[19] P. Dong,[8] J. Donini,[43] T. Dorigo,[43] S. Dube,[52] K. Ebina,[57] J. Efron,[39] J. Ehlers,[19] R. Erbacher,[7] D. Errede,[23] S. Errede,[23] R. Eusebi,[16] H.C. Fang,[28] S. Farrington,[29] I. Fedorko,[46] W.T. Fedorko,[13] R.G. Feild,[60] M. Feindt,[25] J.P. Fernandez,[31] R. Field,[17] G. Flanagan,[48] L.R. Flores-Castillo,[47] A. Foland,[21] S. Forrester,[7] G.W. Foster,[16] M. Franklin,[21] J.C. Freeman,[28] I. Furic,[13] M. Gallinaro,[50] J. Galyardt,[12] J.E. Garcia,[46] M. Garcia Sciveres,[28] A.F. Garfinkel,[48] C. Gay,[60] H. Gerberich,[23] D. Gerdes,[34] S. Giagu,[51] P. Giannetti,[46] A. Gibson,[28] K. Gibson,[12] C. Ginsburg,[16] N. Giokaris,[14] K. Giolo,[48] M. Giordani,[54] P. Giromini,[18] M. Giunta,[46] G. Giurgiu,[12] V. Glagolev,[14] D. Glenzinski,[16] M. Gold,[37] N. Goldschmidt,[34] J. Goldstein,[42] G. Gomez,[11] G. Gomez-Ceballos,[11] M. Goncharov,[53] O. González,[31] I. Gorelov,[37] A.T. Goshaw,[15] Y. Gotra,[47] K. Goulianos,[50] A. Gresele,[43] M. Griffiths,[29] S. Grinstein,[21] C. Grosso-Pilcher,[13] R.C. Group,[17] U. Grundler,[23] J. Guimaraes da Costa,[21] Z. Gunay-Unalan,[35] C. Haber,[28] S.R. Hahn,[16] K. Hahn,[45] E. Halkiadakis,[52] A. Hamilton,[33] B.-Y. Han,[49] J.Y. Han,[49] R. Handler,[59] F. Happacher,[18] K. Hara,[55] M. Hare,[56] S. Harper,[42] R.F. Harr,[58] R.M. Harris,[16] K. Hatakeyama,[50] J. Hauser,[8] C. Hays,[15] A. Heijboer,[45] B. Heinemann,[29] J. Heinrich,[45] M. Herndon,[59] D. Hidas,[15] C.S. Hill,[10] D. Hirschbuehl,[25] A. Hocker,[16] A. Holloway,[21] S. Hou,[1] M. Houlden,[29] S.-C. Hsu,[9] B.T. Huffman,[42] R.E. Hughes,[39] J. Huston,[35] J. Incandela,[10] G. Introzzi,[46] M. Iori,[51] Y. Ishizawa,[55] A. Ivanov,[7] B. Iyutin,[32] E. James,[16] D. Jang,[52] B. Jayatilaka,[34] D. Jeans,[51] H. Jensen,[16] E.J. Jeon,[27] S. Jindariani,[17] M. Jones,[48] K.K. Joo,[27] S.Y. Jun,[12] T.R. Junk,[23] T. Kamon,[53] J. Kang,[34] P.E. Karchin,[58] Y. Kato,[41] Y. Kemp,[25] R. Kephart,[16] U. Kerzel,[25] V. Khotilovich,[53] B. Kilminster,[39] D.H. Kim,[27] H.S. Kim,[27] J.E. Kim,[27] M.J. Kim,[12] S.B. Kim,[27] S.H. Kim,[55] Y.K. Kim,[13] L. Kirsch,[6] S. Klimenko,[17] M. Klute,[32] B. Knuteson,[32] B.R. Ko,[15] H. Kobayashi,[55] K. Kondo,[57] D.J. Kong,[27] J. Konigsberg,[17] A. Korytov,[17] A.V. Kotwal,[15] A. Kovalev,[45] A. Kraan,[45] J. Kraus,[23] I. Kravchenko,[32] M. Kreps,[25] J. Kroll,[45] N. Krumnack,[4] M. Kruse,[15] V. Krutelyov,[53] S. E. Kuhlmann,[2] Y. Kusakabe,[57] S. Kwang,[13] A.T. Laasanen,[48] S. Lai,[33] S. Lami,[46] S. Lammel,[16] M. Lancaster,[30] R.L. Lander,[7] K. Lannon,[39] A. Lath,[52] G. Latino,[46] I. Lazzizzera,[43] T. LeCompte,[2] J. Lee,[49] J. Lee,[27] Y.J. Lee,[27] S.W. Lee,[53] R. Lefèvre,[3] N. Leonardo,[32] S. Leone,[46] S. Levy,[13] J.D. Lewis,[16] C. Lin,[60] C.S. Lin,[16] M. Lindgren,[16] E. Lipeles,[9] T.M. Liss,[23] A. Lister,[19] D.O. Litvintsev,[16] T. Liu,[16] N.S. Lockyer,[45] A. Loginov,[36] M. Loreti,[43] P. Loverre,[51] R.-S. Lu,[1] D. Lucchesi,[43] P. Lujan,[28] P. Lukens,[16] G. Lungu,[17] L. Lyons,[42] J. Lys,[28] R. Lysak,[1] E. Lytken,[48] P. Mack,[25] D. MacQueen,[33] R. Madrak,[16] K. Maeshima,[16] T. Maki,[22] P. Maksimovic,[24] S. Malde,[42] G. Manca,[29] F. Margaroli,[5] R. Marginean,[16] C. Marino,[23] A. Martin,[60] V. Martin,[38] M. Martínez,[3] T. Maruyama,[55] P. Mastrandrea,[51] H. Matsunaga,[55] M.E. Mattson,[58] R. Mazini,[33] P. Mazzanti,[5] K.S. McFarland,[49] M. McFarlane,[28] P. McIntyre,[53] R. McNulty,[29] A. Mehta,[29] S. Menzemer,[11] A. Menzione,[46] P. Merkel,[48] C. Mesropian,[50] A. Messina,[51] M. von der Mey,[8] T. Miao,[16] N. Miladinovic,[6] J. Miles,[32] R. Miller,[35] J.S. Miller,[34] C. Mills,[10]

M. Milnik,[25] R. Miquel,[28] A. Mitra,[1] G. Mitselmakher,[17] A. Miyamoto,[26] N. Moggi,[5] B. Mohr,[8] R. Moore,[16] M. Morello,[46] P. Movilla Fernandez,[28] J. Mülmenstädt,[28] A. Mukherjee,[16] Th. Muller,[25] R. Mumford,[24] P. Murat,[16] J. Nachtman,[16] J. Naganoma,[57] S. Nahn,[32] I. Nakano,[40] A. Napier,[56] D. Naumov,[37] V. Necula,[17] C. Neu,[45] M.S. Neubauer,[9] J. Nielsen,[28] T. Nigmanov,[47] L. Nodulman,[2] O. Norniella,[3] E. Nurse,[30] T. Ogawa,[57] S.H. Oh,[15] Y.D. Oh,[27] T. Okusawa,[41] R. Oldeman,[29] R. Orava,[22] K. Osterberg,[22] C. Pagliarone,[46] E. Palencia,[11] R. Paoletti,[46] V. Papadimitriou,[16] A.A. Paramonov,[13] B. Parks,[39] S. Pashapour,[33] J. Patrick,[16] G. Pauletta,[54] M. Paulini,[12] C. Paus,[32] D.E. Pellett,[7] A. Penzo,[54] T.J. Phillips,[15] G. Piacentino,[46] J. Piedra,[44] L. Pinera,[17] K. Pitts,[23] C. Plager,[8] L. Pondrom,[59] X. Portell,[3] O. Poukhov,[14] N. Pounder,[42] F. Prakoshyn,[14] A. Pronko,[16] J. Proudfoot,[2] F. Ptohos,[18] G. Punzi,[46] J. Pursley,[24] J. Rademacker,[42] A. Rahaman,[47] A. Rakitin,[32] S. Rappoccio,[21] F. Ratnikov,[52] B. Reisert,[16] V. Rekovic,[37] N. van Remortel,[22] P. Renton,[42] M. Rescigno,[51] S. Richter,[25] F. Rimondi,[5] L. Ristori,[46] W.J. Robertson,[15] A. Robson,[20] T. Rodrigo,[11] E. Rogers,[23] S. Rolli,[56] R. Roser,[16] M. Rossi,[54] R. Rossin,[17] C. Rott,[48] A. Ruiz,[11] J. Russ,[12] V. Rusu,[13] H. Saarikko,[22] S. Sabik,[33] A. Safonov,[53] W.K. Sakumoto,[49] G. Salamanna,[51] O. Saltó,[3] D. Saltzberg,[8] C. Sanchez,[3] L. Santi,[54] S. Sarkar,[51] L. Sartori,[46] K. Sato,[55] P. Savard,[33] A. Savoy-Navarro,[44] T. Scheidle,[25] P. Schlabach,[16] E.E. Schmidt,[16] M.P. Schmidt,[60] M. Schmitt,[38] T. Schwarz,[34] L. Scodellaro,[11] A.L. Scott,[10] A. Scribano,[46] F. Scuri,[46] A. Sedov,[48] S. Seidel,[37] Y. Seiya,[41] A. Semenov,[14] L. Sexton-Kennedy,[16] I. Sfiligoi,[18] M.D. Shapiro,[28] T. Shears,[29] P.F. Shepard,[47] D. Sherman,[21] M. Shimojima,[55] M. Shochet,[13] Y. Shon,[59] I. Shreyber,[36] A. Sidoti,[44] P. Sinervo,[33] A. Sisakyan,[14] J. Sjolin,[42] A. Skiba,[25] A.J. Slaughter,[16] K. Sliwa,[56] J.R. Smith,[7] F.D. Snider,[16] R. Snihur,[33] M. Soderberg,[34] A. Soha,[7] S. Somalwar,[52] V. Sorin,[35] J. Spalding,[16] M. Spezziga,[16] F. Spinella,[46] T. Spreitzer,[33] P. Squillacioti,[46] M. Stanitzki,[60] A. Staveris-Polykalas,[46] R. St. Denis,[20] B. Stelzer,[8] O. Stelzer-Chilton,[42] D. Stentz,[38] J. Strologas,[37] D. Stuart,[10] J.S. Suh,[27] A. Sukhanov,[17] K. Sumorok,[32] H. Sun,[56] T. Suzuki,[55] A. Taffard,[23] R. Takashima,[40] Y. Takeuchi,[55] K. Takikawa,[55] M. Tanaka,[2] R. Tanaka,[40] N. Tanimoto,[40] M. Tecchio,[34] P.K. Teng,[1] K. Terashi,[50] S. Tether,[32] J. Thom,[16] A.S. Thompson,[20] E. Thomson,[45] P. Tipton,[49] V. Tiwari,[12] S. Tkaczyk,[16] D. Toback,[53] S. Tokar,[14] K. Tollefson,[35] T. Tomura,[55] D. Tonelli,[46] M. Tönnesmann,[35] S. Torre,[18] D. Torretta,[16] S. Tourneur,[44] W. Trischuk,[33] R. Tsuchiya,[57] S. Tsuno,[40] N. Turini,[46] F. Ukegawa,[55] T. Unverhau,[20] S. Uozumi,[55] D. Usynin,[45] A. Vaiciulis,[49] S. Vallecorsa,[19] A. Varganov,[34] E. Vataga,[37] G. Velev,[16] G. Veramendi,[23] V. Veszpremi,[48] R. Vidal,[16] I. Vila,[11] R. Vilar,[11] T. Vine,[30] I. Vollrath,[33] I. Volobouev,[28] G. Volpi,[46] F. Würthwein,[9] P. Wagner,[53] R. G. Wagner,[2] R.L. Wagner,[16] W. Wagner,[25] R. Wallny,[8] T. Walter,[25] Z. Wan,[52] S.M. Wang,[1] A. Warburton,[33] S. Waschke,[20] D. Waters,[30] W.C. Wester III,[16] B. Whitehouse,[56] D. Whiteson,[45] A.B. Wicklund,[2] E. Wicklund,[16] G. Williams,[33] H.H. Williams,[45] P. Wilson,[16] B.L. Winer,[39] P. Wittich,[16] S. Wolbers,[16] C. Wolfe,[13] T. Wright,[34] X. Wu,[19] S.M. Wynne,[29] A. Yagil,[16] K. Yamamoto,[41] J. Yamaoka,[52] T. Yamashita,[40] C. Yang,[60] U.K. Yang,[13] Y.C. Yang,[27] W.M. Yao,[28] G.P. Yeh,[16] J. Yoh,[16] K. Yorita,[13] T. Yoshida,[41] G.B. Yu,[49] I. Yu,[27] S.S. Yu,[16] J.C. Yun,[16] L. Zanello,[51] A. Zanetti,[54] I. Zaw,[21] F. Zetti,[46] X. Zhang,[23] J. Zhou,[52] and S. Zucchelli[5]

(CDF Collaboration)

[1]*Institute of Physics, Academia Sinica, Taipei, Taiwan 11529, Republic of China*
[2]*Argonne National Laboratory, Argonne, Illinois 60439*
[3]*Institut de Fisica d'Altes Energies, Universitat Autonoma de Barcelona, E-08193, Bellaterra (Barcelona), Spain*
[4]*Baylor University, Waco, Texas 76798*
[5]*Istituto Nazionale di Fisica Nucleare, University of Bologna, I-40127 Bologna, Italy*
[6]*Brandeis University, Waltham, Massachusetts 02254*
[7]*University of California, Davis, Davis, California 95616*
[8]*University of California, Los Angeles, Los Angeles, California 90024*
[9]*University of California, San Diego, La Jolla, California 92093*
[10]*University of California, Santa Barbara, Santa Barbara, California 93106*
[11]*Instituto de Fisica de Cantabria, CSIC-University of Cantabria, 39005 Santander, Spain*
[12]*Carnegie Mellon University, Pittsburgh, PA 15213*
[13]*Enrico Fermi Institute, University of Chicago, Chicago, Illinois 60637*
[14]*Joint Institute for Nuclear Research, RU-141980 Dubna, Russia*
[15]*Duke University, Durham, North Carolina 27708*
[16]*Fermi National Accelerator Laboratory, Batavia, Illinois 60510*
[17]*University of Florida, Gainesville, Florida 32611*
[18]*Laboratori Nazionali di Frascati, Istituto Nazionale di Fisica Nucleare, I-00044 Frascati, Italy*
[19]*University of Geneva, CH-1211 Geneva 4, Switzerland*
[20]*Glasgow University, Glasgow G12 8QQ, United Kingdom*
[21]*Harvard University, Cambridge, Massachusetts 02138*

[22]Division of High Energy Physics, Department of Physics,
University of Helsinki and Helsinki Institute of Physics, FIN-00014, Helsinki, Finland
[23]University of Illinois, Urbana, Illinois 61801
[24]The Johns Hopkins University, Baltimore, Maryland 21218
[25]Institut für Experimentelle Kernphysik, Universität Karlsruhe, 76128 Karlsruhe, Germany
[26]High Energy Accelerator Research Organization (KEK), Tsukuba, Ibaraki 305, Japan
[27]Center for High Energy Physics: Kyungpook National University,
Taegu 702-701, Korea; Seoul National University, Seoul 151-742,
Korea; and SungKyunKwan University, Suwon 440-746, Korea
[28]Ernest Orlando Lawrence Berkeley National Laboratory, Berkeley, California 94720
[29]University of Liverpool, Liverpool L69 7ZE, United Kingdom
[30]University College London, London WC1E 6BT, United Kingdom
[31]Centro de Investigaciones Energeticas Medioambientales y Tecnologicas, E-28040 Madrid, Spain
[32]Massachusetts Institute of Technology, Cambridge, Massachusetts 02139
[33]Institute of Particle Physics: McGill University, Montréal,
Canada H3A 2T8; and University of Toronto, Toronto, Canada M5S 1A7
[34]University of Michigan, Ann Arbor, Michigan 48109
[35]Michigan State University, East Lansing, Michigan 48824
[36]Institution for Theoretical and Experimental Physics, ITEP, Moscow 117259, Russia
[37]University of New Mexico, Albuquerque, New Mexico 87131
[38]Northwestern University, Evanston, Illinois 60208
[39]The Ohio State University, Columbus, Ohio 43210
[40]Okayama University, Okayama 700-8530, Japan
[41]Osaka City University, Osaka 588, Japan
[42]University of Oxford, Oxford OX1 3RH, United Kingdom
[43]University of Padova, Istituto Nazionale di Fisica Nucleare,
Sezione di Padova-Trento, I-35131 Padova, Italy
[44]LPNHE, Universite Pierre et Marie Curie/IN2P3-CNRS, UMR7585, Paris, F-75252 France
[45]University of Pennsylvania, Philadelphia, Pennsylvania 19104
[46]Istituto Nazionale di Fisica Nucleare Pisa, Universities of Pisa,
Siena and Scuola Normale Superiore, I-56127 Pisa, Italy
[47]University of Pittsburgh, Pittsburgh, Pennsylvania 15260
[48]Purdue University, West Lafayette, Indiana 47907
[49]University of Rochester, Rochester, New York 14627
[50]The Rockefeller University, New York, New York 10021
[51]Istituto Nazionale di Fisica Nucleare, Sezione di Roma 1,
University of Rome "La Sapienza," I-00185 Roma, Italy
[52]Rutgers University, Piscataway, New Jersey 08855
[53]Texas A&M University, College Station, Texas 77843
[54]Istituto Nazionale di Fisica Nucleare, University of Trieste/ Udine, Italy
[55]University of Tsukuba, Tsukuba, Ibaraki 305, Japan
[56]Tufts University, Medford, Massachusetts 02155
[57]Waseda University, Tokyo 169, Japan
[58]Wayne State University, Detroit, Michigan 48201
[59]University of Wisconsin, Madison, Wisconsin 53706
[60]Yale University, New Haven, Connecticut 06520

(Dated: June 3, 2006)

We present a measurement of the top quark pair production cross section in $p\overline{p}$ collisions at $\sqrt{s} = 1.96$ TeV using 318 pb^{-1} of data collected with the Collider Detector at Fermilab. We select $t\overline{t}$ decays into the final states $e\nu$ + jets and $\mu\nu$ + jets, in which at least one b quark from the t-quark decays is identified using a secondary vertex-finding algorithm. Assuming a top quark mass of 178 GeV/c^2, we measure a cross section of $8.7 \pm 0.9(\text{stat.})^{+1.1}_{-0.9}(\text{syst.})$ pb. We also report the first observation of $t\overline{t}$ with significance greater than 5σ in the subsample in which both b quarks are identified, corresponding to a cross section of $10.1^{+1.6}_{-1.4}(\text{stat.})^{+2.0}_{-1.3}(\text{syst.})$ pb.

PACS numbers: 14.65.Ha, 13.85.Ni, 13.85.Qk

The top quark completes the third quark generation in the Standard Model (SM). Due to its large mass, nearly 40 times greater than that of the next heaviest quark, the top quark can at present only be studied at the Fermilab Tevatron, a $p\overline{p}$ collider with a center-of-mass energy ($\sqrt{s}$) of 1.96 TeV. In these collisions, the SM top

quark is mostly produced in pairs through $q\overline{q}$ annihilation and gluon fusion with a total theoretical cross section of $6.1^{+0.6}_{-0.8}$ pb [1] for a mass of 178 GeV/c^2 [2]. Previous measurements of the $t\overline{t}$ production cross section ($\sigma_{t\overline{t}}$) performed at the Tevatron [3, 4] were consistent with SM expectations, but suffered from large uncertainties due to small event samples. With significant enhancements in the integrated luminosity and our sensitivity to t-quark decay products, we are no longer limited by statistical uncertainties, now reaching a precision comparable to that of the theory.

The top quark decays predominantly to a W boson and a bottom quark. We expect the top quark signal significance to be greatest in the lepton+jets channel, in which top quark pairs decay through the chain $t\overline{t} \to W^+W^-b\overline{b} \to \ell\nu q\overline{q}'b\overline{b}$. A typical $t\overline{t}$ event in this decay channel will include an electron or muon with large transverse momentum (p_T), four jets corresponding to the four final-state quarks, and an imbalance in the total transverse energy in the event ($\not\!\!E_T$) from the undetected neutrino [5]. We distinguish $t\overline{t}$ events from background by requiring at least one jet to be identified as a bottom quark (b-tagged) using the secondary vertex-finding algorithm (`SecVtx`) described in Ref. [3]. We have reoptimized the algorithm to enhance the efficiency for b-tagging two jets per event; the sample of events with this signature is dominated by $t\overline{t}$ ($> 90\%$ pure), making it an ideal environment for direct determination of top quark properties. In this Letter, we present a measurement of the $t\overline{t}$ cross section ($\sigma_{t\overline{t}}$) in b-tagged lepton+jets events, and we also report the first observation of $t\overline{t}$ with significance greater than 5σ in doubly b-tagged events.

Results reported here are obtained using 318 pb^{-1} of integrated luminosity collected between March 2002 and August 2004 by the Collider Detector at Fermilab (CDF II). The CDF II detector [6] is a general-purpose particle detector located at one of the two interaction points at the Tevatron Collider. Inside a 1.4 T solenoidal magnetic field, a large open-cell drift chamber, the Central Outer Tracker (COT) [7], and an eight-layer silicon system [8] provide tracking information. The COT covers the pseudo-rapidity range $|\eta| < 1.1$ and provides a long lever arm for track curvature measurements. The silicon system provides three-dimensional hit information between radii of 1.3 cm and 28 cm, with an $r - \phi$ impact parameter resolution of $\sim 40\mu$m (including a 30 μm contribution from the beamspot). Outside the solenoid, electromagnetic and hadronic calorimeters surround the tracking volume in a projective tower geometry, identifying jets and electrons with $|\eta| < 3.6$. Electron energies are measured in the central electromagnetic calorimeter for $|\eta| < 1.1$ and in the end-plug calorimeters for $1.1 < |\eta| < 3.6$. Beyond the calorimeters, drift chambers provide muon identification in the region $|\eta| < 1.0$.

The data were collected with an inclusive high-p_T lepton trigger that requires an electron (muon) with transverse energy $E_T > 18$ GeV ($p_T > 18$ GeV/c). The trigger efficiency, including lepton identification, is $95.9 \pm 1.5\%$ ($87.7 \pm 1.5\%$) for electrons (muons). Following the event selection used in Ref. [3], we require all leptons to be isolated [9] and $E_T > 20$ GeV ($p_T > 20$ GeV/c) for electrons (muons). We remove events with multiple high-p_T leptons, a cosmic ray muon, a photon conversion electron, or a track that forms the Z mass with the lepton. The position of the primary vertex along the beam is required to be within 60 cm of the nominal interaction position and consistent with the z position of the high-p_T lepton.

After leptons are selected, we require the presence of at least three jets with $|\eta| < 2$ and $E_T > 15$ GeV (E_T is corrected as described in Ref. [10]). Jets are clustered with a cone-based algorithm with a cone size $\Delta R \equiv \sqrt{\Delta\phi^2 + \Delta\eta^2} = 0.4$.

To account for the expected neutrino, we require large missing transverse energy, $\not\!\!E_T > 20$ GeV. The invariant mass of the lepton and the neutrino, with the longitudinal neutrino momentum set to zero, is required to exceed 20 GeV/c^2; this rejects $\sim 50\%$ of background events that do not contain a real W boson. Finally, as $t\overline{t}$ events typically have larger total transverse energy than background events, we require that the scalar sum of the $\not\!\!E_T$ and the lepton and total jet transverse energies (H_T) be greater than 200 GeV. This leaves 310 (190) events in the electron (muon) data sample, dominated by W bosons with associated production of light-flavor jets ($W+$ LF). Table I includes the event count before b-tagging (pretag) sorted by the number of jets in the event. The one- and two-jet bins have been included as an assumed control sample, although without the H_T requirement.

We improve the $t\overline{t}$ signal significance by requiring at least one jet to be b-tagged with the `SecVtx` algorithm [3]. Due to their long lifetime, b quarks typically decay a measurable distance from the primary interaction point. We reconstruct the decay vertices using a minimum of two or three tracks with an impact parameter significance greater than 3.0 or 2.0, respectively. Contributions from K^0_S and Λ decays and interactions in the inner detector material are reduced through additional requirements on the invariant mass of the secondary vertex and an upper limit on the track impact parameter, $d_0 < 0.15$ cm. We measure the two-dimensional displacement of the secondary vertex from the primary interaction point projected along the jet axis (L_{2D}); a jet is b-tagged if the vertex has L_{2D} significance larger than 6.0. The probability of misidentifying a light-flavor jet as a b-quark jet due to detector resolution (mistag rate) is estimated from secondary vertices reconstructed behind the primary vertex with L_{2D} significance less than -6.0.

The $t\overline{t}$ acceptance is calculated from a combination of data and Monte Carlo simulation. We use the PYTHIA Monte Carlo generator [11] with CTEQ5L parton distribution functions [12] and assume $M_{top} = 178$ GeV/c^2, the world average top quark mass measurement from

Run I [2]. The CLEO QQ Monte Carlo program [13] models the decays of bottom and charm hadrons. These events are passed through a GEANT [14] simulation of the CDF II detector and subjected to the same selection requirements as the data. The total acceptance, including the branching fraction, is calculated as the product of geometric and kinematic acceptances (including lepton identification) and the trigger efficiency. The efficiency to identify isolated high-p_T leptons in the simulation is scaled to the value measured in $Z \to \ell^+\ell^-$ data. The acceptance for electron (muon) events before b-tagging is $3.8 \pm 0.3\%$ ($2.8 \pm 0.2\%$).

The b-tagging efficiency for the full $t\bar{t}$ event is measured in a $t\bar{t}$ simulation that has been tuned to match the single jet b-tagging efficiency in the data. A multiplicative scale factor ($S_b = 0.927 \pm 0.066$), measured in heavy-flavor-enriched samples of non-isolated, low-E_T leptons, corrects for the per-jet efficiency difference between data and simulation [3]. In $t\bar{t}$ events, we measure a b-tagging efficiency of $48 \pm 4\%$ for b-quark jets with a corresponding mistag rate of $1.2 \pm 0.1\%$; we therefore expect $69 \pm 5\%$ ($23 \pm 3\%$) of these events to have at least one b-tag (two b-tags).

The systematic uncertainty in the cross section due to the S_b correction is 6%, dominated by the extrapolation from the charm-contaminated low-E_T sample to more energetic $t\bar{t}$ events. Other leading systematic uncertainties arise from the integrated luminosity measurement (6%) [16], jet energy corrections (5%), lepton isolation (2%), lepton identification (2%), parton distribution functions (2%), choice of Monte Carlo generator (2%), and modeling of initial and final state radiation (1%).

The background to $t\bar{t}$ is mostly due to direct production of a W boson with multiple jets (W+jets). Smaller contributions come from QCD jet production in which the W signature is faked by jets appearing as electrons or by semi-leptonic b-hadron decays (non-W), and electroweak processes such as single top quark production, diboson (WW, WZ, and ZZ) production, and Z boson decays to tau pairs. We describe these backgrounds in turn and summarize the results in Tables I and II.

We separate the contribution from W+jets into events with and without heavy-flavor jets. For the former, the fractions of W+jets events attributable to $Wb\bar{b}$, $Wc\bar{c}$, and Wc are estimated with ALPGEN/HERWIG Monte Carlo [17, 18], then scaled by a multiplicative factor of 1.5 ± 0.4 to reproduce the b-tag rates observed in a control sample of inclusive jet data. The expected number of events is estimated by multiplying these fractions by the number of pretag events, after removing the pretag expectations for all other backgrounds and $t\bar{t}$ signal.

We estimate the background contribution from W events with only light-flavor jets by applying the mistag rate, measured in the inclusive jet dataset and parameterized in jet E_T, η, ϕ, and number of tracks and the total jet energy in the event, to the lepton+jets dataset. The mistag rate is adjusted higher by $36 \pm 13\%$ to account for heavy-flavor contamination in the jet data and residual contributions from material interactions and K^0_S/Λ decays. Finally, this result is adjusted down by the fraction of the data sample attributed to physics processes with heavy-flavor production.

The expectation for the non-W background is determined using data. Assuming that the isolation of the lepton and the $\not\!\!E_T$ in these events are uncorrelated [3], we extrapolate from the low-$\not\!\!E_T$ and non-isolated regions (which contain fewer real W bosons) to predict the non-W content of the pretag and signal sample.

Finally, we use Monte Carlo to estimate the backgrounds due to single top (PYTHIA/MADEVENT [15]) and dibosons/$Z \to \tau\tau$ (PYTHIA), normalizing the expectations to their respective theoretical cross sections [19]. Here, the b-tagging efficiency is evaluated analogously to the $t\bar{t}$ signal prediction.

Backgrounds that depend on the assumed $t\bar{t}$ cross section are calculated iteratively. The signal and background contributions to the b-tagged data sample, sorted by jet multiplicity, are summarized in Table I and Figure 1(a). The total corrected background in the signal region with at least one b-tag is 46 ± 9 events, where we observe 174 events. We interpret the excess of events with three or more jets as pure $t\bar{t}$ signal, corresponding to a cross section of $8.7 \pm 0.9(\text{stat.})^{+1.1}_{-0.9}(\text{syst.})$ pb.

We observe 54 events with multiple b-tags, the first time the event yield is inconsistent with the no-top hypothesis with significance greater than 5σ. After correcting for $t\bar{t}$, we expect 4.1 ± 2.5 background events, a significant improvement in signal purity (Table III). We summarize these results in Table II and Figure 1(b); the agreement in five-jet events underscores our ability to model initial- and final-state gluon radiation. We measure a cross section of $10.1^{+1.6}_{-1.4}(\text{stat.})^{+2.0}_{-1.3}(\text{syst.})$ pb in the multiply b-tagged sample, consistent with the result for events with a single b-tag.

The acceptance and efficiency both have a small dependence on the top quark mass; the cross section measurements change by ± 0.08 pb for each ∓ 1 GeV/c^2 change in the assumed top quark mass from the initial value of 178 GeV/c^2, in the range of 160 – 190 GeV/c^2.

We perform two cross checks using alternate b-tagging algorithms. Table III compares the b-tagging characteristics of these checks with those of the main analyses. In the first, we repeat the analysis with an update of the original `SecVtx` algorithm described in Ref. [3] (`TSecVtx`). We observe 138 events with at least one b-tag, over an expected background of 25 ± 5 events. The measured cross section is $8.7 \pm 0.9(\text{stat.})^{+1.1}_{-0.9}(\text{syst.})$ pb. In the second cross check, we use the `Jet Probability` algorithm [20]. We observe 120 events with at least one b-tag compared to a background of 21 ± 3 events, corresponding to $\sigma_{t\bar{t}} = 8.9 \pm 1.0(\text{stat.})^{+1.1}_{-1.0}(\text{syst.})$ pb. Both cross checks are in agreement with the lead result above,

albeit with highly correlated uncertainties.

In summary, we have measured a $t\bar{t}$ production cross section of $8.7 \pm 0.9(\text{stat.})^{+1.1}_{-0.9}(\text{syst.})$ pb in $p\bar{p}$ collisions at $\sqrt{s} = 1.96$ TeV using 318 pb^{-1} of data with at least one secondary vertex b-tag. The result is consistent with the SM expectation of $6.1^{+0.6}_{-0.8}$ pb for a top quark mass of 178 GeV/c^2, which changes by ± 0.2 pb for every ∓ 1 GeV/c^2 shift in the assumed mass. Additionally, we have studied a large, very pure sample of $t\bar{t}$ events with at least two b-tags, which will form the foundation for future high-precision measurements of top quark properties. In this sample, we measure $\sigma_{t\bar{t}} = 10.1^{+1.6}_{-1.4}(\text{stat.})^{+2.0}_{-1.3}(\text{syst.})$ pb.

We thank the Fermilab staff and the technical staffs of the participating institutions for their vital contributions. This work was supported by the U.S. Department of Energy and National Science Foundation; the Italian Istituto Nazionale di Fisica Nucleare; the Ministry of Education, Culture, Sports, Science and Technology of Japan; the Natural Sciences and Engineering Research Council of Canada; the National Science Council of the Republic of China; the Swiss National Science Foundation; the A.P. Sloan Foundation; the Bundesministerium für Bildung und Forschung, Germany; the Korean Science and Engineering Foundation and the Korean Research Foundation; the Particle Physics and Astronomy Research Council and the Royal Society, UK; the Russian Foundation for Basic Research; the Comisión Interministerial de Ciencia y Tecnología, Spain; in part by the European Community's Human Potential Programme under contract HPRN-CT-2002-00292; and the Academy of Finland.

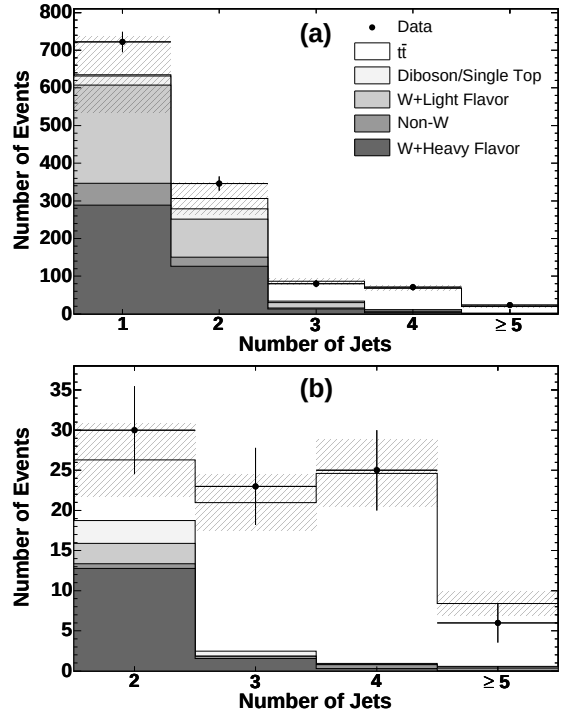

FIG. 1: Summary of background and signal event yields versus number of jets in the event when requiring (a) at least one b-tagged jet and (b) at least two b-tagged jets. The $t\bar{t}$ contribution is normalized to the measured cross section in each sample. The H_T requirement is released for events with fewer than 3 jets. The hashed region shows the uncertainty on the total expectation.

[1] N. Kidonakis and R. Vogt, Phys. Rev. D **68**, 114014 (2003); M. Cacciari *et al.*, J. High Energy Phys. **0404**, 68 (2004).

[2] CDF and DØ Collaborations, hep-ex/0404010.

[3] D. Acosta *et al.* (CDF Collaboration), Phys. Rev. D **71**, 052003 (2005).

[4] D. Acosta *et al.* (CDF Collaboration), Phys. Rev. Lett. **93**, 142001 (2004); Phys. Rev. D **52**, 052003 (2005); **71**, 072005 (2005); V.M. Abazov *et al.* (DØ Collaboration), Phys. Lett. B **626**, 35 (2005); **626**, 45 (2005); **626**, 55 (2005).

[5] We use a cylindrical coordinate system about the beam axis in which θ is the polar angle, ϕ is the azimuthal angle, and $\eta \equiv -\ln\tan(\theta/2)$. $E_T \equiv E \sin\theta$ and $p_T \equiv p\sin\theta$ where E is the energy measured in the calorimeter and p is the momentum measured by the spectrometer. The missing E_T ($\vec{\not{E}}_T$) is defined by $\vec{\not{E}}_T = -\sum_i E_T^i \hat{n}_i$, where i = calorimeter tower number with $|\eta| < 3.6$ and $\hat{n}_i$ is a unit vector perpendicular to the beam axis and pointing at the ith calorimeter tower. We also define $\not{E}_T = |\vec{\not{E}}_T|$.

[6] F. Abe *et al.* (CDF Collaboration), Nucl. Instrum. Methods A **271**, 387 (1988); D. Acosta *et al.* (CDF Collaboration), Phys. Rev. D **71**, 032001 (2005).

[7] T. Affolder *et al.*, Nucl. Instrum. Methods A **526**, 249 (2004).

[8] A. Sill *et al.*, Nucl. Instrum. Methods A **447**, 1 (2000).

[9] We require the calorimeter transverse energy in a cone of $\Delta R \equiv \sqrt{\Delta\eta^2 + \Delta\phi^2} < 0.4$ around the lepton (not including the lepton itself) divided by the electron (muon) transverse energy (momentum) to be less than 0.1.

[10] Raw jet energies are corrected for detector effects (tower-by-tower variations), η-dependent response, and multiple $p\bar{p}$ collisions in an event. Details on the correction methods may be found in A. Bhatti *et al.*, submitted to Nucl. Instrum. Methods A, hep-ex/0510047.

[11] T. Sjöstrand *et al.*, Comput. Phys. Commun. **76**, 361 (1993); TP 01-21, LU (2001), hep-ph/0108264. We use version 6.2.

[12] J. Pumplin *et al.*, J. High Energy Phys. **0207**, 012 (2002).

[13] P. Avery, K. Read, and G. Trahern, Cornell Internal Note CSN-212, 1985 (unpublished). We use version 9.1.

[14] R. Brun and F. Carminati, CERN Programming Library Long Writeup **W5013** (1993).

[15] T. Stelzer and W.F. Long, Comput. Phys. Commun. **81**, 337 (1994).

[16] D. Acosta *et al.*, Nucl. Instrum. Methods A **494**, 57 (2002); S. Klimenko, J. Konigsberg, and T.M. Liss, FERMILAB-FN-0741 (2003).

TABLE I: Summary of event yields and background (Bkgd) expectations sorted by the number of jets in the event. Event totals before b-tagging (Pretag) are listed in the first row; all other entries correspond to the sample with at least one b-tagged jet, assuming the measured $t\bar{t}$ cross section of 8.7 pb. The H_T requirement is released for events with fewer than 3 jets.

	$W+1$ jet	$W+2$ jets	$W+3$ jets	$W+4$ jets	$W+\geq 5$ jets
Pretag	30,283	4676	324	142	34
Dibosons	6.3 ± 0.9	11.8 ± 1.7	1.7 ± 0.3	0.46 ± 0.12	0.15 ± 0.04
t	8.1 ± 2.9	13.2 ± 4.0	1.8 ± 0.5	0.39 ± 0.12	0.08 ± 0.03
$Z \to \tau\tau$	9.7 ± 1.9	2.5 ± 0.5	0.18 ± 0.04	0.017 ± 0.003	0.008 ± 0.002
$Wb\bar{b}$	114 ± 35	63 ± 19	6.1 ± 1.6	1.4 ± 0.7	0.17 ± 0.09
$Wc\bar{c}$	46 ± 13	30 ± 9	3.8 ± 1.2	1.1 ± 0.4	0.13 ± 0.04
Wc	128 ± 33	34 ± 9	3.0 ± 0.8	0.81 ± 0.21	0.10 ± 0.03
$W+LF$	261 ± 57	101 ± 22	14.4 ± 3.2	4.4 ± 1.0	0.61 ± 0.13
Non-W	58 ± 12	24 ± 5	2.8 ± 0.7	2.5 ± 0.8	0.20 ± 0.18
Bkgd	632 ± 100	279 ± 43	33.6 ± 5.8	11.1 ± 2.4	1.43 ± 0.59
$t\bar{t}$	3.5 ± 0.4	27.9 ± 3.2	52.9 ± 5.8	56.7 ± 6.1	18.2 ± 2.0
Total	635 ± 100	307 ± 43	86.5 ± 8.2	67.9 ± 6.6	19.6 ± 2.1
Data	722	346	80	71	23

TABLE II: Summary of event yields and background (Bkgd) expectations sorted by the number of jets in the event, for events with at least two b-tagged jets, assuming the measured $t\bar{t}$ cross section of 10.1 pb. The H_T requirement is released for events with 2 jets. The $Z \to \tau\tau$ background is negligible.

	$W+2$ jets	$W+3$ jets	$W+4$ jets	$W+\geq 5$ jets
Dibosons	0.68 ± 0.12	0.11 ± 0.02	0.041± 0.010	0.017 ± 0.005
t	2.2 ± 0.5	0.53 ± 0.15	0.12 ± 0.04	0.026 ± 0.010
$Wb\bar{b}$	11.3 ± 3.6	1.3 ± 0.4	0.21 ± 0.08	0.010 ± 0.004
$Wc\bar{c}$	0.92 ± 0.41	0.22 ± 0.11	0.07 ± 0.04	0.003 ± 0.002
Wc	0.51 ± 0.15	0.05 ± 0.03	0.021 ± 0.012	0.001 ± 0.001
$W+LF$	2.5 ± 1.3	0.02 ± 0.11	0.00 ± 0.12	0.16 ± 0.23
Non-W	0.59 ± 0.59	0.28 ± 0.28	0.5 ± 0.5	0.35 ± 0.35
Bkgd	18.7 ± 4.3	2.5 ± 1.2	1.0 ± 0.8	0.6 ± 0.5
$t\bar{t}$	7.5 ± 1.3	18.5 ± 3.2	23.7 ± 4.1	7.9 ± 1.4
Total	26.3 ± 4.5	21.0 ± 3.4	24.6 ± 4.2	8.4 ± 1.4
Data	30	23	25	6

TABLE III: Summary of b-tagging information for the algorithms used, where ϵ_b is the b-tagging efficiency for b-quark jets in $t\bar{t}$ events and $\epsilon_b^{t\bar{t}}$ is the per-event efficiency for $t\bar{t}$.

	SecVtx		TSecVtx	Jet Probability
ϵ_b (%)	48 ± 4		40 ± 3	35 ± 3
Mistag rate (%)	1.20 ± 0.07		0.48 ± 0.04	1.22 ± 0.08
b-tags per event	≥ 1	≥ 2	≥ 1	≥ 1
$\epsilon_b^{t\bar{t}}$ (%)	69 ± 5	23 ± 3	60 ± 3	54 ± 4
Observed $\frac{Signal}{Background}$	2.8	12.2	4.5	4.7

[17] M.L. Mangano *et al.*, J. High Energy Phys. **0307**, 001 (2003).

[18] G. Marchesini and B.R. Webber, Nucl. Phys. **B310**, 461 (1988); G. Marchesini *et al.*, Comput. Phys. Commun. **67**, 465 (1992); G. Corcella *et al.*, J. High Energy Phys. **0101**, 010 (2001). We use version 6.4.

[19] J. Campbell and R. Ellis, Phys. Rev. D **60**, 113006 (1999); B. Harris *et al.*, Phys. Rev. D **66**, 054024 (2002).

[20] T. Affolder *et al.* (CDF Collaboration), Phys. Rev. D **64**, 032002 (2001); A. Abulencia *et al.* (CDF Collaboration), to be submitted to PRD (updated CDF result).